FEBS Letters

FEBS PRESS science publishing by scientists

Integrins and heparan sulfate proteoglycans on hepatic stellate cells (HSC) are novel receptors for HSC-derived exosomes

Li Chen[1] and David R. Brigstock[1,2]

1 The Research Institute at Nationwide Children's Hospital, Columbus, OH, USA
2 Department of Surgery, Wexner Medical Center, The Ohio State University, Columbus, OH, USA

Correspondence
D. R. Brigstock, Room WA2011, Research Building 2, Nationwide Children's Hospital, 700 Children's Drive, Columbus OH 43205, USA
Fax: 614 722 5892
Tel: 614 355 2824
E-mail: David.Brigstock@Nationwide Childrens.Org

(Received 25 May 2016, revised 22 September 2016, accepted 22 September 2016, available online 23 October 2016)

doi:10.1002/1873-3468.12448

Edited by Lukas Alfons Huber

Exosomes mediate intercellular microRNA delivery between hepatic stellate cells (HSC), the principal fibrosis-producing cells in the liver. The purpose of this study was to identify receptors on HSC for HSC-derived exosomes, which bind to HSC rather than to hepatocytes. Our findings indicate that exosome binding to HSC is blocked by treating HSC with RGD, EDTA, integrin αv or β1 siRNAs, integrin αvβ3 or α5β1 neutralizing antibodies, heparin, or sodium chlorate. Furthermore, exosome cargo delivery and exosome-regulated functions in HSC, including expression of fibrosis- or activation-associated genes and/or miR-214 target gene regulation, are dependent on cellular integrin αvβ3, integrin α5β1, or heparan sulfate proteolgycans (HSPG). Thus, integrins and HSPG mediate the binding of HSC-derived exosomes to HSC as well as the delivery and intracellular action of the exosomal payload.

Keywords: connective tissue growth factor; fibrogenesis; hepatic fibrosis; microRNA; microvesicle

Hepatic stellate cells (HSC) account for 3–5% of the cells in the liver and, under normal circumstances, are a quiescent cell type that plays a role in vitamin A storage and regulation of vascular tone [1]. During liver injury, HSC undergo an activation process that results in important alterations in their phenotype and function that are central to wound healing, including enhanced proliferation, migration, increased contractility due to expression of α smooth muscle actin (αSMA), and production of matrix proteins (collagen) [2]. In acute injury, this activation is transient and results in the deposition of a provisional matrix scaffold to support hepatocyte proliferation and repopulation. Chronic liver injury leads to a perpetuation of the activated HSC phenotype resulting in unabated collagen production, causing fibrous scar material to be deposited which, over time, can seriously impede normal liver function [3]. Fibrogenic pathways in activated HSC are mediated by transforming growth factor-beta or connective tissue growth factor (CCN2; also known as CTGF) which are produced by activated HSC as well as by other liver cell types after injury [1–6]. Pathways of fibrogenesis in HSC have become the focus of a concerted effort to understand the underlying mechanisms involved and have led to the identification of rational targets for therapeutic intervention [7–10]; the importance of these advances is underscored by the paucity of approved antifibrotic drugs despite the prevalence of liver fibrosis, which affects millions of people globally.

Connective tissue growth factor production in quiescent HSC is directly suppressed by the binding to the

Abbreviations
CCN2, connective tissue growth factor; HSC, hepatic stellate cell; HSPG, heparan sulfate proteoglycans; miR, microRNA; siRNA, small interfering RNA; αSMA, alpha smooth muscle actin; UTR, untranslated region.

CCN2 3′-UTR of microRNA (miR) -214 or miR-199a-5p each of which is transcribed downstream of the Twist1 transcription factor [11–13]. This inhibitory Twist1-miR-214-miR-199a-5p pathway is suppressed in activated HSC, allowing CCN2 to be produced and to drive fibrogenesis in the cells. Twist1 or miR-214/199a-5p may also be exported from HSC in exosomes [11–13], membranous nanovesicles that arise by inward budding of multivesicular bodies and which are released extracellularly when multivesicular bodies fuse internally with the plasma membrane. Exosomes traverse the intercellular space and may be taken up by neighboring cells, including HSC themselves [14]. Exosomes contain a complex mixture of miRs, mRNA and proteins that reflect the transcriptional and/or translational activity of the donor cell and which may cause epigenetic reprogramming and phenotypic alterations in recipient cells [14–16]. Exosomes from quiescent HSC are intercellularly shuttled to activated HSC in which the activated phenotype is then suppressed [12,13,17]. This is due, in part, to exosomal delivery of Twist1 or miR-214/199a-5p that cause, respectively, enhanced expression of miR-214 or reduced expression of CCN2, the net effect of which is to dampen CCN2-dependent fibrogenic pathways in activated HSC [12,13,17]. Similarly, CCN2 can also be exosomally shuttled from activated HSC and delivered to other HSC recipients in which it is biologically active and can drive fibrogenesis [18]. Collectively, the participation of neighboring HSC in exosomal communication networks represents a mechanism by which fibrogenic signaling is fine-tuned and up- or down-regulated according to the differential activation status of recipient and donor cells. Despite these advances, exosomes represent a largely unexplored component of fibrogenic signaling that requires detailed study.

Exosomal cargo transfer between HSC occurs as a result of the direct binding of exosomes to the surface of the recipient HSC. An improved understanding of the molecular basis for exosome interactions with target HSC may provide unique opportunities to exploit this natural delivery mechanism for improving efficacy or targeting of antifibrotic agents. The purpose of these studies was to identify cell surface molecules that mediate functional binding of HSC-derived exosomes to recipient HSC.

Materials and methods

Animal procedures

Animal protocols were approved by the Institutional Animal Care and Use Committee of Nationwide Children's Hospital (Columbus, OH, USA). Male FVB mice (6–8 weeks) (n = 10) were injected intraperitoneally three times each week for 5 weeks with either 30 μL of vegetable oil or a mixture of 0.5 μL carbon tetrachloride (CCl_4; Sigma-Aldrich, St Louis, MO, USA) in 29.5 μL of vegetable oil. Mice were then injected via the tail vein with 40 μg of PKH26-labeled HSC-derived exosomes and 4 h later, animals were sacrificed. Livers lobes were either perfused for subsequent isolation of HSC or hepatocytes, or immediately harvested along with the other major body organs for fluorescence imaging using a Xenogen IVIS 200 (PerkinElmer, Waltham, MA, USA).

Primary mouse HSC or hepatocytes

Livers from exosome-treated mice were perfused *in situ* and then subjected to either collagenase digestion for isolation of hepatocytes [19] or pronase/collagenase digestion and buoyant-density centrifugation for isolation of HSC [17]. Hepatocytes or HSC were maintained in, respectively, complete William E medium (Gibco, Billings, MT, USA) or DMEM/F12/10% FBS for 24 h and then analyzed by confocal microscopy for the presence of PKH26.

For *in vitro* exosome binding studies, hepatocytes or HSC were isolated from Swiss Webster mice as described above and maintained in primary culture for up to, respectively, 72 h or passage 6 (P6; 1 : 3 split every 5 days). Binding assays were performed on cells seeded at 5000 cells/well in 8-well multi-chamber slides (Falcon, Caroll, OH, USA).

Purification of HSC-derived exosomes

Exosomes were removed from FBS by serial ultracentrifugation [20] prior to using it for HSC culture. Exosomes were isolated from conditioned medium of P6 HSC using standardized steps of low and ultraspeed centrifugation [20]. Nanoparticle tracking analysis (Nanosight™, Malvern Instruments, Westborough, MA, USA) was used to determine exosome size and frequency. Exosomes were further evaluated for morphology and size using a Tecnai G2 F20 cryogenic transmission electron microscope (FEI; Hillsboro, Oregon, OR, USA) as described [17]. For some experiments, HSC were treated with 500 nM SYTO RNASelect™ Green Fluorescent Cell Stain (Thermo Fisher Scientific, Waltham, MA, USA) for 12 h and then incubated in fresh medium (exosome-free) for 48 h prior to exosome isolation. For other experiments, miR-199a-5p mimic (Qiagen, Germantown, MD, USA) was labeled with Cy3 dye using a Label IT® miRNA labeling kit (Mirus Bio LLC, Madison, WI, USA) and then transfected into exosomes by electroporation using a Nucleofector kit (Lonza, Koln, Germany); exosomes were then repurified using a PureExo kit (101Bio, Palo Alto, CA, USA).

Exosome binding assays

Exosomes from control or SYTO-RNA-labeled HSC or that contained Cy3-miR-199a-5p were labeled for 1 h with 4 μM of the fluorescent lipophilic membrane dyes PKH26 or PKH67, according the manufacturer's specifications (Sigma-Aldrich). Exosomes (0–4 $\mu g \cdot mL^{-1}$) or free Cy3-labeled miR-199a-5p (1 μM) were added for up to 48 h to primary mouse HSC or hepatocytes which were then washed in PBS and imaged using a confocal microscope (Zeiss, Obercochen, Germany) or lysed in lysis buffer (Boston Bioproducts, Ashland, MA, USA) and measured at 590/540 nm using a Spectra Max® M2 microplate reader (VWR, Atlanta, GA, USA) to assess levels of PKH26 fluorescence. Prior to exosome addition in some experiments, HSC were stained with PKH67 (Sigma-Aldrich) and hepatocytes were stained with far red (Sigma-Aldrich). In some binding experiments, HSC were pretreated or coincubated with 0–100 $\mu g \cdot mL^{-1}$ RGD or RGE tripeptides (American Peptide, Sunnyvale, CA, USA), 0–100 μM EDTA (Sigma-Aldrich), 0–10 μM sodium chlorate (Sigma-Aldrich), 0–10 μM sodium sulfate (Sigma-Aldrich), 0–10 $\mu g \cdot mL^{-1}$ rabbit anti-mouse integrin αvβ3 IgG (Bioss Inc, Woburn, MA, USA), or 0–20 $\mu g \cdot mL^{-1}$ rat anti-mouse integrin α5β1 IgG (Millipore, Temecula, CA, USA) or 0–10 $\mu g \cdot mL^{-1}$ rat anti-mouse integrin αM, (CD11b; Novus Biologicals, Littleton, CO, USA). For antibody studies, nonimmune IgG was used as a negative control.

Integrin knockdown

Small interfering RNA (siRNA) to mouse integrin αv or β1, or negative controls were purchased from Santa Cruz Biotechnology (Santa Cruz, CA, USA). To avoid off-target effects, the siRNA preparations consisted of three target-specific 20–25 nucleotide siRNA. Primary mouse HSC (10^5–10^6 cells) were transfected with 100 nM siRNA by electroporation using a Nucleofector Kit (Lonza) and incubated for 12 h in medium containing 10% FBS which was then replaced with fresh medium. Our previous data have shown a 40% transfection efficiency of siRNA in primary mouse HSC using this approach [12]. Integrin knockdown was confirmed by RT-PCR (see Table 1 for primer sequences) or western blot analysis of cell lysates using anti-αvβ3 or anti-α5β1 with anti-β-actin (Abcam, Cambridge, MA, USA) serving as a loading control [12,13,17]. Cells were then used for exosome binding analysis as described above.

Regulation of CCN2-3′UTR by miR-214-enriched exosomes

The full-length 997 bp 3′-UTR of mouse CCN2 was subcloned into a Fire-Ctx sensor lentivector (SBI, Mountain View, CA, USA), downstream of the *Firefly* luciferase reporter and cytotoxin (*CTX*) drug sensor genes as described [17]. Recipient HSC were transfected with parental or CCN2 3′-UTR vectors for 24 h prior to 1-h incubation with RGD, IgG, anti-integrin αvβ3 or anti-integrin α5β1. Cells were then incubated for 24 h in the presence of exosomes isolated from Day 1 HSC which we previously showed are highly enriched in miR-214 which directly targets the CCN2 3′-UTR [17]. To control transfection efficiency, the cells were also transfected with 0.8 μg pRL-CMV vector (Promega, Madison, WI, USA) containing *Renilla* luciferase reporter gene. Luciferase activity was measured in triplicate using an E1910 Dual Luciferase Reporter Assay System (Promega). *Renilla* luciferase activity was used for normalization, and Firefly luciferase activity in exosome-treated cells was compared to that in nontreated cells.

HSC coculture system

One well of a 2-well microculture system (Ibidi Inc., Verona, WI, USA) [12,13,17] received exosome donor P6 HSC that had been transfected with 100 nM pre-mir-214 (Life Technologies, Carlsbad, CA, USA). Some cells were cultured with 10 μM GW4869, an inhibitor of neutral sphingomyelinase 2 which is required for exosome biogenesis [21,22]. After 12 h, the other well was seeded with P6 HSC transfected with parental miR-Selection Fire-Ctx lentivector or the same vector containing either wild-type or mutant CCN2 3′-UTR lacking the miR-214 binding site [17]. After 12 h, direct communication between the cells was initiated and proceeded for 24 h. In some experiments, 100 $\mu g \cdot mL^{-1}$ heparin sulfate or 100 $\mu g \cdot mL^{-1}$ chondroitin sulfate were included in the culture medium. Luciferase activity was measured in triplicate using the Dual Luciferase Reporter Assay System. Firefly luciferase activity in pre-mir-21-transfected cells was compared to that in nontransfected cells, with *Renilla* luciferase activity used for normalization.

Table 1. Primers used for RT-PCR.

Gene	Genbank accession number	Sense primer	Antisense primer	Product size (bp)
Integrin αv (mouse)	NM_008402	5′-ACATCACCTGGGGCATTCAG-3′	5′-GTGAACTTGGAGCGGACAGA-3′	251
Integrin β1 (mouse)	NM_010578	5′-AATGTTTCAGTGCAGAGCC-3′	5′-TTGGGATGATGTCGGGAC-3′	254
GAPDH (mouse)	NM_002046	5′-TGCACCACCAACTGCTTAGC-3′	5′-GGCATGGACTGTGGTCATGAG-3′	87

Cell adhesion assay

Ninety-six-well nontissue culture plates (Costar, Corning, NY, USA) were coated with CCN2 and blocked with BSA prior to addition of 50 μL cell suspension (2.5×10^5 cells·mL^{-1}) for 30 mins at 37 °C as described [23]. The added cells were primary mouse activated HSC (see above) or Day 9 primary mouse bone-marrow-derived macrophages that were obtained as described [24]. Prior to addition to the CCN2-coated wells, cells were preincubated for 30 mins with 10–20 μg·mL^{-1} anti-integrin antibodies or nonimmune IgG. Wells were washed three times with PBS and adherent cells were fixed with 10% formalin and quantified using CyQUANT GR dye [23].

Immunoctyochemistry

P6 HSC were treated for 36 h with or without exosomes (8 μg·mL^{-1}) from D1-3 HSC in the presence or absence of anti-integrin αvβ3 or anti-integrin α5β1. Cells were fixed and incubated with NH1 anti-CCN2 IgY (5 μg·mL^{-1} [25]), anti-αSMA (1 : 100; Dako Cytomation, Glostrup, Denmark) or anti-collagen α(1) (1 : 250; Abcam), followed by Alexa Fluor® 568 goat-anti chicken IgY, Alexa Fluor® 647 goat anti-(mouse IgG), or Alexa Fluor® 488 goat anti-(rabbit IgG), respectively. The cells were mounted with Vectashield Mounting Medium containing 4′,6-diamidino-2-phenylindole (DAPI) nuclear stain (Vector Laboratories, Burlingame, CA, USA), and examined by confocal microscopy.

Heparin-affinity

One hundred micrograms of HSC exosomes were added to 120 μL TSKgel heparin-5PW affinity beads (Tosoh BioScience LLC, King of Prussia, PA, USA) in 200 μL PBS and mixed at 37 °C for 1 h. The beads were washed three times with 1 mL PBS and then split into 10 equal aliquots which were then mixed for 15 mins with 200 μL PBS containing 0.15–2.5 M NaCl. The beads were collected by centrifugation, washed twice in 200 μL of their respective NaCl treatment, and then extracted into 20 μL 2× SDS/PAGE sample buffer, with boiling for 5 mins. 18 μL of each sample was subjected to SDS/PAGE and analyzed by western blot with anti-CD81 (Pro-Sci, Fort Collins, CO, USA), using a chemiluminscent detection kit (Promega) to visualize immunoreactive protein.

Statistical analysis

Data from binding assays, RT-PCR, western blots, cellular fluorescence or luciferase activity assays are reported as the mean ± SEM. Statistical significance was analyzed using Student's *t*-test and $P < 0.05$ was considered statistically significant. All statistical analyses were performed using SIGMA PLOT 12.0 software (SPSS Inc., Chicago, IL, USA).

Results

Cellular binding of HSC-derived exosomes

Exosomes isolated from P6 mouse HSC had a mean diameter of 144 nm as assessed by nanoparticle tracking analysis and were bimembrane vesicles as assessed by cryogenic transmission electron microscopy (Fig. 1A). These features were consistent with our earlier reports in which we demonstrated HSC exosomes to have a mean diameter of 140 nm as assessed by dynamic light scattering, to carry a net charge of −26 mV, and to express the exosome markers, CD9, CD81, and flotillin-1 [12,13,17]. Exosomes were then labeled with the lipophilic fluorescent dye PKH26 so that their interactions with target cells could be visualized and quantified. As shown in Fig. 1B, exosome binding to HSC was detected within 1 h and reached maximal levels by 12 h, with approximately 50% of binding occurring at 3–6 h. Exosomes from activated HSC demonstrated a dose-dependent binding to HSC recipient cells (Fig. 1C) that resulted in delivery into the cells of their RNA cargo which became separated from the exosomal membrane components between 5 and 24 h after addition to the cells (Fig. 1D). Uptake into recipient cells of exosomal miR-199a-5p similarly resulted in its distinct localization in the cells as compared to exosomal membrane stain and was effectively delivered into the cells, unlike free miR-199a-5p (Fig. 1E). Exosomes bound strongly to primary cultures of HSC but not to hepatocytes, a phenomenon that was apparent in either individual cultures of each cell type, or in cocultures of both cell types (Fig. 1F). To verify that these findings faithfully reflected the preferential binding of exosomes to activated HSC *in vivo*, we analyzed the hepatic localization of systemically injected exosomes. As shown in Fig. 1G, within 4 h of tail vein injection, exosomes had accumulated mainly within CCl_4-injured livers to the exclusion of the other organ systems. Examination of isolated liver cells from control or CCl_4-treated mice revealed that the exosomes had bound to the HSC population, with essentially nondetectable binding to hepatocytes (Fig. 1H). Based on their preferential binding to HSC both *in vitro* and *in vivo*, subsequent binding studies of HSC-derived exosomes were performed using activated HSC *in vitro*.

Role of integrins in exosome binding to HSC

Binding of exosomes to HSC was dose-dependently blocked by inclusion of RGD in the incubation medium during a 12-h binding experiment, the specificity

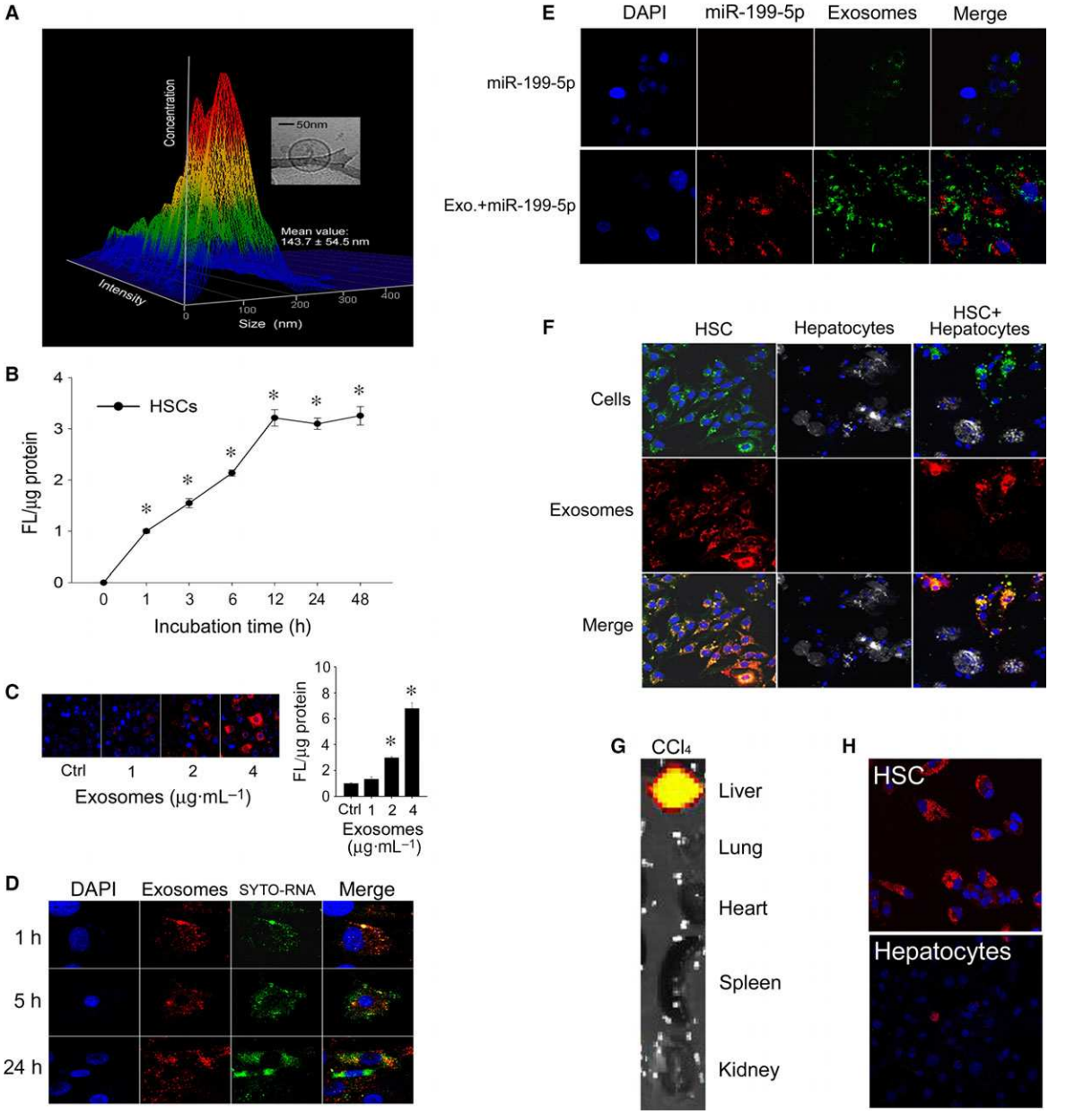

Fig. 1. Characterization of HSC-derived exosomes and their preferential binding to HSC. (A) Nanoparticle tracking analysis of exosomes secreted by P6 mouse HSC, showing a size range of 144 ± 55 nm. The inset shows the typical spherical bimembrane characteristic of the exosomes as assessed by cryogenic transmission electron microscopy. (B) PKH26-stained exosomes from mouse HSC were incubated with primary mouse HSC for 0–48 h. Cell-associated fluorescence, assessed by spectrophotometry of cell lysates, was significant by 1 h and reached maximal levels by 12 h. $n = 5$, $^*P < 0.001$ versus 0 h; student's *t*-test. (C) Dose-dependent binding of exosomes to HSC over 24 h. The figure shows confocal microscopy of a representative experiment (left) and quantification of cell-associated fluorescence (right). $n = 5$ $^*P < 0.001$ versus Ctrl; student's *t*-test. 'Ctrl' is no added exosomes. (D) HSC were incubated with PKH26-labeled exosomes (red) containing SYTO-RNA (green) and the distribution of fluorescence in the cells was examined after 1, 5 or 24 h. Blue, 4′,6-diamidino-2-phenylindole. Data shown are representative of three replicates. (E) HSC were incubated for 24 h with Cy3-labeled miR-199a-5p (red) either free in solution or after electroporation into PKH67-labeled exosomes (green). Data shown are representative of three replicates. (F) PKH26-stained exosomes (red) from mouse HSC were incubated for 5 h with PKH67-stained primary mouse P6 HSC (green; 1st column), fluorescence far red-stained primary mouse hepatocytes (grey; 2nd column) or a coculture of both cell types (3rd column). Blue, 4′,6-diamidino-2-phenylindole. Data shown are representative of three replicates. (G) Distribution of PKH26-stained HSC-derived exosomes 4 h after i.v. injection in CCl_4-treated mice. Data shown are representative of five animals. (H) Representative fluorescence imaging of HSC or hepatocytes isolated from the mice in (G).

of which was demonstrated by the inability of RGE to block exosome binding (Fig. 2A). Preincubation of the target HSC for 1 h with RGD, followed by extensive rinsing to remove excess peptide, also resulted in reduced exosome binding, whereas preincubation with RGE was ineffective (Fig. 2B). Since the RGD-sensitivity and specificity of exosome binding suggested a possible involvement of cell surface integrins, many of which require divalant cations for function, binding experiments were also performed in the presence of EDTA with the result that 50–100 μM EDTA inhibited exosome binding to HSC over 24 h (Fig. 2C). To address the possible functional role of integrins αv or β1, HSC were transfected with siRNA to either or both subunits for 24 h prior to incubation with exosomes for the subsequent 24 h. This treatment, which resulted in decreased levels of αv or β1 mRNA of 78% or 75%, respectively, and of αv or β1 protein levels of 75% or 90%, respectively (Fig. 2D), caused > 95% of exosome binding to be blocked by the siRNAs, either individually or collectively (Fig. 2E). Since we have previously documented the expression and function of integrins αvβ3 or α5β1 in activated HSC [23,26], we examined their possible role in exosome binding. We first confirmed the functionality of neutralizing anti-integrin αvβ3 or anti-integrin α5β1 antibodies by demonstrating that they blocked adhesion of HSC to CCN2 as previously reported [23,26] (Fig. 2F). We next showed that these antibodies also caused a dose-dependent decrease in exosome binding, with > 90% inhibition at 4 $\mu g \cdot mL^{-1}$ anti-αvβ3 or 20 $\mu g \cdot mL^{-1}$ anti-α5β1 (Fig. 2G). The specificity of this outcome was confirmed using an antibody to integrin αM which neither blocked exosome binding to HSC (Fig. 2G) nor HSC binding to CCN2 (Fig. 2F) but nonetheless blocked macrophage adhesion to CCN2 (Fig. 2F) consistent with the absence of integrin αM in quiescent or activated HSC [27] and the role of integrin αM as a CCN2 adhesion receptor for macrophages [28,29]. Collectively, the antibody neutralization studies demonstrated a specific functional role for integrin αvβ3 and integrin α5β1 in mediating exosome binding to HSC.

The inhibitory action of exosomal miR-214 on CCN2 3′-UTR activity [17] was blocked by RGD, anti-integrin αvβ3 or anti-integrin α5β1, but not by nonimmune IgG (Fig. 2H). Furthermore, the ability of exosomes from quiescent HSC to suppress production of αSMA, collagen 1(α1), or CCN2 in activated HSC was also blocked by anti-integrin αvβ3 or anti-integrin α5β1 (Fig. 2I). Collectively, these data show that cell surface integrins αvβ3 or α5β1 are required for exosomal delivery of regulatory miRs into HSC and downstream phenotypic reprogramming in the recipient cells, which includes inhibition of activation- and fibrosis-associated gene expression.

Fig. 2. Integrin-dependency of exosome interactions with HSC. (A) PKH26-stained HSC-derived exosomes (red) were incubated with primary mouse HSC for 24 h in the presence of RGD or RGE (0–100 $\mu g \cdot mL^{-1}$) in the incubation medium. Cells were analyzed by confocal microscopy (20×) (*upper*, showing a representative experiment) or measured for cell-associated fluorescence by spectrophotometry of cell lysates (*lower; n = 5,* $*P < 0.001$ versus 0 $\mu g \cdot mL^{-1}$ RGD, student's *t*-test). (B) Mouse HSC were preincubated with RGD or RGE (0–100 $\mu g \cdot mL^{-1}$) for 1 h and excess peptide was removed by extensive washing prior to addition of PKH26-stained HSC exosomes (red) for 24 h. The cells were analyzed by confocal microscopy (20×) (*upper;* showing a representative experiment) or by fluorescence intensity of cell lysates *(lower; n* = 5, $*P < 0.001$ versus 0 $\mu g \cdot mL^{-1}$ RGD, student's *t*-test). (C) PKH26-stained exosomes (red) were incubated with primary mouse HSC (green) for 24 h with 0–100 μM EDTA. Cells were analyzed by confocal microscopy (20×) (*left*; showing a representative experiment) or fluorescence in cell lysates was determined spectrophotometrically (*right*; *n* = 5, $*P < 0.001$ versus 0 μM EDTA, student's *t*-test). (D) HSC were transfected for 24 h with integrin αv or β1 siRNA and analyzed for expression of αv or β1 mRNA by RT-PCR (left; *n* = 9, $*P < 0.001$ versus Ctrl, student's *t*-test) or levels of their corresponding proteins by western blot using anti-integrin αvβ3 (center) or anti-integrin α5β1 antibodies (right) for which β-actin was used a loading control (*n* = 9, $*P < 0.001$ versus Ctrl, student's *t*-test). 'Ctrl' represents cells treated with a scrambled siRNA sequence. (E) Mouse HSC were transfected for 24 h with siRNA to the integrin αv or β1 subunits, either individually or together. Cells were then stained with PKH-67 (green) for 1 h and incubated with PKH26-stained exosomes (red) for 24 h. Blue, 4′,6-diamidino-2-phenylindole. Data are representative of three experiments. (F) Adhesion of mouse HSC or macrophages to a CCN2 substrate after preincubation of the cells with neutralizing anti-integrin αvβ3 (10 $\mu g \cdot mL^{-1}$), anti-integrin α5β1 (20 $\mu g \cdot mL^{-1}$), anti-integrin αM (10 $\mu g \cdot mL^{-1}$), or their nonimmune IgG counterparts (at the same respective dose). *n* = 5, $*P < 0.001$ versus Ctrl, student's *t*-test. (G) Mouse HSC were preincubated with neutralizing anti-integrin αvβ3, α5β1 or αM IgG or nonimmune IgG for 1 h prior to addition for 24 h of PKH26-stained HSC exosomes. Cells were analyzed by confocal microscopy (20×) (*upper*, showing a representative experiment) or by spectrophotometric quantification of fluorescence in cell lysates (*lower*, *n* = 6, $*P < 0.001$. $+P < 0.05$ versus Ctrl, student's *t*-test). (H) Recipient HSC were transfected with a parental or CCN2 3′-UTR luciferase reporter vector for 24 h prior to 1-h incubation with RGD, IgG, anti-integrin αvβ3, or anti-integrin α5β1. Cells were then incubated for 24 h in the presence of miR-214-enriched exosomes as described [17]. Exosome-mediated suppression of luciferase activity was inhibited by RGD or anti-integrin αvβ3. *n* = 9, $*P < 0.001$ versus Ctrl, student's *t*-test. (I) Immunocytochemical detection of CCN2, αSMA or collagen α1 in activated HSC alone ('Ctrl') or after 36-h incubation with exosomes from D1-3 HSC, in the presence or absence of anti-integrin αvβ3 or anti-integrin α5β1. Data are representative of three experiments.

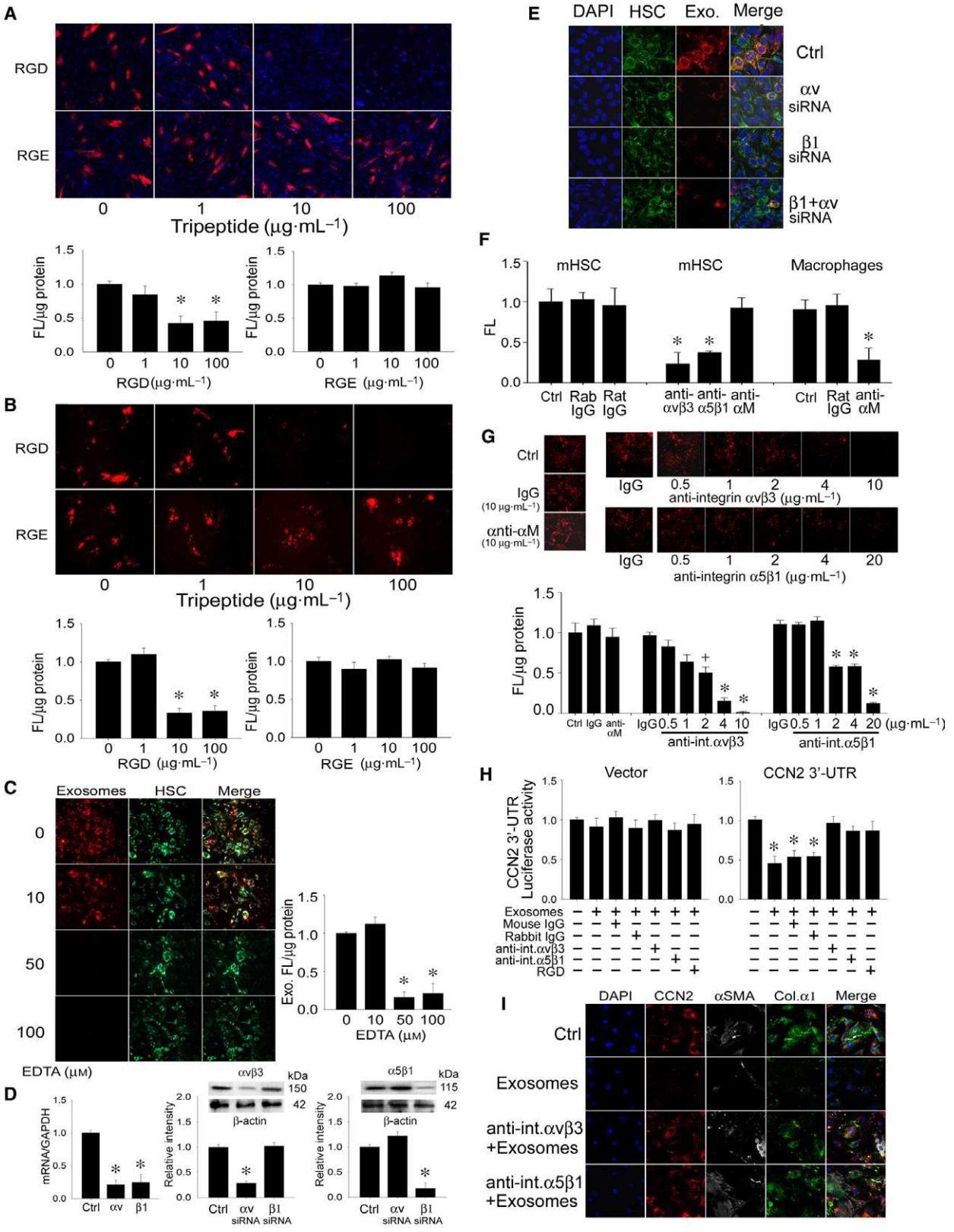
A
RGD
RGE
0 1 10 100
Tripeptide (μg·mL−1)
FL/μg protein
RGD(μg·mL−1)
RGE (μg·mL−1)
B
RGD
RGE
Tripeptide (μg·mL−1)
RGD (μg·mL−1)
RGE (μg·mL−1)
C
Exosomes HSC Merge
EDTA (μM)
Exo. FL/μg protein
D
mRNA/GAPDH
Ctrl αv β1
αvβ3 kDa 150 42 β-actin
α5β1 kDa 115 42 β-actin
Relative intensity
siRNA siRNA
E
DAPI HSC Exo. Merge
Ctrl
αv siRNA
β1 siRNA
β1+αv siRNA
F
mHSC mHSC Macrophages
FL
Ctrl Rab IgG Rat IgG anti-αvβ3 anti-α5β1 anti-αM Ctrl Rat IgG anti-αM
G
Ctrl
IgG (10 μg·mL−1)
αnti-αM (10 μg·mL−1)
IgG 0.5 1 2 4 10
anti-integrin αvβ3 (μg·mL−1)
IgG 0.5 1 2 4 20
anti-integrin α5β1 (μg·mL−1)
FL/μg protein
Ctrl IgG anti-αM
anti-int.αvβ3
anti-int.α5β1
H
Vector
CCN2 3'-UTR
CCN2 3'-UTR Luciferase activity
Exosomes
Mouse IgG
Rabbit IgG
anti-int.αvβ3
anti-int.α5β1
RGD
I
DAPI CCN2 αSMA Col.α1 Merge
Ctrl
Exosomes
anti-int.αvβ3 +Exosomes
anti-int.α5β1 +Exosomes

Role of cell surface heparin-like molecules in exosome binding to HSC

As shown in Fig. 3A, incubation of exosomes with HSC was inhibited in a dose-dependent manner when heparin sulfate, but not chondroitin sulfate, was included in the incubation medium. Furthermore, pretreatment of the HSC with sodium chlorate to selectively reduce sulfation of heparan sulfate proteoglycans (HSPG) resulted in an inhibition of exosome binding (Fig. 3B). This outcome was reversed by coincubation of the cells with sodium sulfate to rescue them from the chlorate block (Fig. 3B). Finally, the biological significance of HSPG-exosome interactions

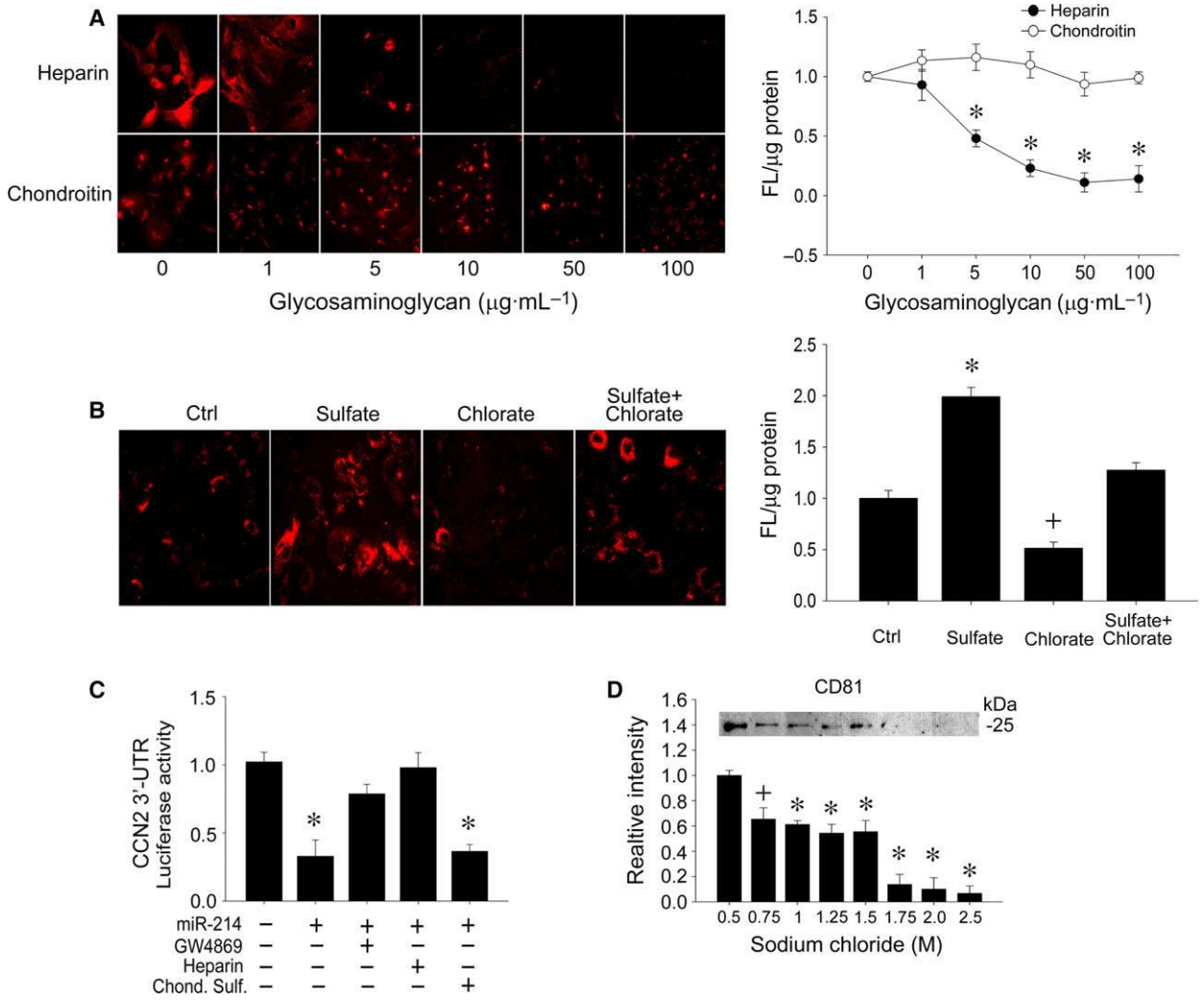

Fig. 3. Heparin-dependency of exosome interactions with HSC. (A) PKH26-stained exosomes (red) were incubated with primary mouse HSC for 24 h in the presence of 0–100 μg·mL^{-1} heparin or chondroitin sulfate. Cells were analyzed by confocal microscopy (20×) (*left*; showing a representative experiment) or fluorescence intensity of cell lysates by spectrophotometry (*right*; $n = 5$, $^*P < 0.001$ versus 0 μg·mL^{-1} heparin, student's *t*-test). (B) PKH26-stained exosomes (red) were incubated with primary mouse HSC for 24 h after 24-h pretreatment of the cells with sodium chlorate (10 mM) ± sodium sulfate (10 mM). Cells were analyzed by confocal microscopy (20×) (*left*; showing a representative experiment) or fluorescence intensity of cell lysates by spectrophotometry (*right*; $n = 5$, $^*P < 0.001$; $^+P < 0.05$ versus Ctrl, student's *t*-test). (C) Donor HSC were transfected with miR-214 and cocultured with CCN2 3′-UTR luciferase reporter-transfected recipient HSC for 24 h. Some wells also received GW4869 (10 μM; exosome inhibitor), heparin sulfate (100 μg·mL^{-1}) or chondroitin sulfate (100 μg·mL^{-1}). The inhibition of CCN2 3′-UTR activity by miR-214-enriched exosomes was reversed by GW4869 or heparin, but not by chondroitin sulfate. $n = 9$, $^*P < 0.001$ versus ctrl, student's *t*-test. (D) Heparin-affinity beads were mixed with exosomes (1 h, room temp) prior to washing in PBS and mixing with different NaCl concentrations. The figure shows the extraction of residual exosomes from the heparin beads using sample buffer as assessed by SDS/PAGE and western blot for the exosome-specific marker, CD81. The CD81 signal was not affected by 0–0.5 M NaCl (data not shown). $n = 6$, $^*P < 0.001$; $^+P < 0.05$ versus 0.5 M NaCl, student's *t*-test.

was determined using a HSC-HSC coculture system that allows exosomal communication between neighboring HSC to be examined under normal conditions of endogenous exosome production and action [12,17]. As we have reported [17], coculture of miR-214-transfected donor HSC with CCN2 3′-UTR luciferase reporter-transfected recipient HSC resulted in miR-214-dependent regulation of the CCN2 3′-UTR reporter, the exosome-dependency of which was shown by the ability of the exosome inhibitor, GW4869, to reverse the suppressed CCN2 3′-UTR activity (Fig. 3C). Addition of heparin sulfate to the coculture also reversed miR-214-suppressed CCN2 3′-UTR activity, whereas chondroitin sulfate was ineffective showing that exosomal cargo signaling in the recipient cells was heparin-dependent. Collectively, these data show that downstream cell surface HSPG on HSC are functional receptors for HSC-derived exosomes. To confirm the heparin-binding property of exosomes, they were incubated with heparin-affinity beads in a cell-free system with the result that they bound strongly and required ~ 1.0 M NaCl for their efficient elution (Fig. 3D).

Discussion

In this study, we identified integrins and HSPG as cell surface molecules that are required for binding of HSC-derived exosomes to HSC. Specifically, we showed that integrin αvβ3 or α5β1 in HSC is required for exosome binding, miR uptake, and functional reprogramming in the cells. This represents a novel function for integrin αvβ3 in HSC which has previously been shown to support cell survival, adhesion to CCN2, periostin-dependent activation, and osteopontin-dependent collagen up-regulation [23,26,30–32], all of which reflect the enhanced expression and a central role for integrin αv or αvβ3 in HSC function and hepatic fibrosis [33–35]. Similarly, integrin α5β1 in activated HSC is associated with cell adhesion to fibronectin or CCN2, or fibronectin-dependent survival, cytoskeletal rearrangements or expression of matrix metalloproteases or collagen I [26,36–39], but its role in binding and mediating functional effects of HSC-derived exosomes is novel. Integrin β1 on HSC also engages exosomes from liver sinusoidal endothelial cells [40] suggesting that exosomes from different cell types may compete for common integrin receptors on the same target HSC. Also, we cannot yet exclude the possibility that exosome binding involves either other β1 integrins (e.g. integrin αvβ1 or α8β1, which are RGD-sensitive and expressed by HSC [41,42]) or other RGD-sensitive integrins (e.g. integrins αvβ5, αvβ6, αvβ8, or IIbβ3). Integrin αLβ2 on $CD8^+$ dendritic cells or activated T cells was shown to engage ICAM-1 on dendritic cell-secreted exosomes [43,44] but other studies have demonstrated a role for exosomal integrins in interacting with target cells [45–53] so it will be of interest in the future to determine if exosomal integrins also contribute to exosome-HSC binding interactions.

Heparan sulfate proteolgycans are a family of proteins substituted with glycosaminoglycan polysaccharides that interact broadly with diverse extracellular ligands, although their precise functional interactions are predominantly determined by the extent and site of side chain sulfation [54–56]. HSPG regulate cell growth, proliferation, adhesion, motility and signaling through their ability to act as high capacity low affinity coreceptors for many ligands that are consequently able to interact more efficiently with their specific cognate high affinity receptors [57,58]. Cell surface HSPG bound to HSC-derived exosomes as evidenced by the competition studies in which exosome binding to HSC was blocked by coincubation with heparin sulfate or by preincubation of recipient HSC with sodium chlorate which selectively reduces sulfation of HSPG glycan chains during their biosynthesis in the Golgi apparatus by competitively binding to 3′-phosphoadenosine-5′-phosphosulfate synthase at the active site [59,60]. This effect is reversible in the presence of excess sodium sulfate, a characteristic that allowed the chlorate-induced block of exosome binding to HSC to be rescued. Overall, these data demonstrate a requirement for HSPG sulfation for exosome binding and the cellular (rather than exosomal) localization of the HSPG component. While cell surface HSPG in HSC play a functional role in binding CCN2 by acting as coreceptors in association with integrin αvβ3, integrin α5β1, or low density lipoprotein receptor-related protein [23,26,61], our data reveal an additional role for HSPG in HSC as functional exosome receptors that are required for the downstream action of exosomal miR-214 in target HSC. These findings are similar to the heparin-dependent binding of U-87 glioblastoma cell-derived exosomes to U-87 or CHO cells [62], although our results show that heparin-binding mechanisms are not restricted to exosomes from cancer cells. Since activated human HSC synthesize the HSPG core proteins syndecans 1–4, perlecan, and glypican [63] and syndecan-2 and glypican-1 are associated with internalized glioblastoma exosomes in U-87 cells [62], it will be of interest in future studies to determine which HSPG core proteins are involved in HSC exosome binding.

While we have identified integrin αvβ3, integrin α5β1, and HSPG as important receptors for HSC-derived exosomes and portals for exosomal cargo uptake, the involvement of these molecules in the

highly specific localization of HSC-derived exosomes to HSC in HSC-hepatocyte cocultures *in vitro* or to HSC in fibrotic liver *in vivo* remains to be established. That said, integrin αvβ3 expression in activated HSC has been mechanistically exploited for selective targeting of candidate antifibrotic or cytotoxic agents in experimental liver fibrosis [64–66]. The intrinsic specificity of HSC-derived exosomes for HSC suggests that such exosomes, or the molecular binding partners on their outer surface, may be exploited for targeted delivery of therapeutic drugs to activated HSC in fibrotic livers. Similar translational applications have been proposed for delivery of drugs with targeted actions to cancer cells using the HSPG-binding properties of cancer cell-derived exosomes [62]. Continued analysis of the binding partners involved in the interaction of HSC-derived exosomes with their target HSC will yield important information about the underlying mechanisms involved and their potential for use in targeted drug delivery. Furthermore, continued characterization of suppressive signaling molecules (including but not limited to miR-214 and miR-199a-5p) in exosomes from quiescent HSC offers a new direction for identifying novel antifibrotic agents.

Acknowledgements

This work was supported by NIH grants R01AA021276 and R21AA023626 awarded to DRB. We thank Ruju Chen and Sherri Kemper for their technical assistance, Dr Min Gao (Liquid Crystal Institute, Kent State University, Kent OH) for help with cryogenic transmission electron microscopy, Dr Brian Becknell (Center for Clinical and Translational Research, Nationwide Children's Hospital, Columbus OH) for providing mouse macrophages, and Dr Yongjie Miao (Biostatistics Shared Resource, Nationwide Children's Hospital, Columbus OH) for assistance with statistical analysis.

Author contributions

LC was involved in study concept and design, acquisition of data, analysis and interpretation of data, critical reading of the manuscript, figure preparation; DRB contributed toward study concept and design, analysis and interpretation of data, manuscript preparation, obtained funding, study supervision.

References

1 Friedman SL (2008) Hepatic fibrosis – overview. *Toxicology* **254**, 120–129.
2 Friedman SL (2008) Mechanisms of hepatic fibrogenesis. *Gastroenterology* **134**, 1655–1669.
3 Puche JE, Saiman Y and Friedman SL (2013) Hepatic stellate cells and liver fibrosis. *Compr Physiol* **3**, 1473–1492.
4 Gressner AM and Weiskirchen R (2006) Modern pathogenetic concepts of liver fibrosis suggest stellate cells and TGF-beta as major players and therapeutic targets. *J Cell Mol Med* **10**, 76–99.
5 Gressner AM, Weiskirchen R, Breitkopf K and Dooley S (2002) Roles of TGF-beta in hepatic fibrosis. *Front Biosci* **7**, d793–d807.
6 Huang G and Brigstock DR (2012) Regulation of hepatic stellate cells by connective tissue growth factor. *Front Biosci* **17**, 2495–2507.
7 Friedman SL (2015) Hepatic fibrosis: emerging therapies. *Dig Dis* **33**, 504–507.
8 Lee YA, Wallace MC and Friedman SL (2015) Pathobiology of liver fibrosis: a translational success story. *Gut* **64**, 830–841.
9 Wang P, Koyama Y, Liu X, Xu J, Ma HY, Liang S, Kim IH, Brenner DA and Kisseleva T (2016) Promising therapy candidates for liver fibrosis. *Front Physiol* **7**, 47.
10 Yoon YJ, Friedman SL and Lee YA (2016) Antifibrotic therapies: where are we now? *Semin Liver Dis* **36**, 87–98.
11 Chen L, Charrier A and Brigstock DR (2013) MicroRNA-214-mediated suppression of connective tissue growth factor (CTGF) in hepatic stellate cells is associated with stimulation of miR-214 promoter activity by cellular or exosomal Twist-1. *Hepatology* **58** 4 (Suppl), Abstract 28, 221A.
12 Chen L, Chen R, Kemper S, Charrier A and Brigstock DR (2015) Suppression of fibrogenic signaling in hepatic stellate cells by Twist1-dependent microRNA-214 expression: role of exosomes in horizontal transfer of Twist1. *Am J Physiol Gastrointest Liver Physiol* **309**, G491–G499.
13 Chen L, Chen R, Velazquez VM and Brigstock DR (2016) Fibrogenic signaling is suppressed in hepatic stellate cells through targeting of connective tissue growth factor (CCN2) by cellular or exosomal microRNA-199a-5p. *Am J Pathol* doi: 10.1016/j.ajpath.2016.07.011.
14 Thery C (2011) Exosomes: secreted vesicles and intercellular communications. *F1000 Biol Rep* **3**, 15.
15 Thery C, Ostrowski M and Segura E (2009) Membrane vesicles as conveyors of immune responses. *Nat Rev Immunol* **9**, 581–593.
16 Thery C, Zitvogel L and Amigorena S (2002) Exosomes: composition, biogenesis and function. *Nat Rev Immunol* **2**, 569–579.
17 Chen L, Charrier A, Zhou Y, Chen R, Yu B, Agarwal K, Tsukamoto H, Lee LJ, Paulaitis ME and Brigstock DR (2014) Epigenetic regulation of connective tissue growth factor by MicroRNA-214 delivery in exosomes from mouse or human hepatic stellate cells. *Hepatology* **59**, 1118–1129.

18 Charrier A, Chen R, Chen L, Kemper S, Hattori T, Takigawa M and Brigstock DR (2014) Exosomes mediate intercellular transfer of pro-fibrogenic connective tissue growth factor (CCN2) between hepatic stellate cells, the principal fibrotic cells in the liver. *Surgery* **156**, 548–555.
19 Ghosh A and Sil PC (2006) A 43-kDa protein from the leaves of the herb *Cajanus indicus* L. modulates chloroform induced hepatotoxicity in vitro. *Drug Chem Toxicol* **29**, 397–413.
20 Thery C, Amigorena S, Raposo G and Clayton A (2006) Isolation and characterization of exosomes from cell culture supernatants and biological fluids. *Curr Protoc Cell Biol* **Chapter 3**, Unit 3 22.
21 Chairoungdua A, Smith DL, Pochard P, Hull M and Caplan MJ (2010) Exosome release of beta-catenin: a novel mechanism that antagonizes Wnt signaling. *J Cell Biol* **190**, 1079–1091.
22 Kosaka N, Iguchi H, Yoshioka Y, Takeshita F, Matsuki Y and Ochiya T (2010) Secretory mechanisms and intercellular transfer of microRNAs in living cells. *J Biol Chem* **285**, 17442–17452.
23 Gao R and Brigstock DR (2004) Connective tissue growth factor (CCN2) induces adhesion of rat activated hepatic stellate cells by binding of its C-terminal domain to integrin alphavbeta3 and heparan sulfate proteoglycan. *J Biol Chem* **279**, 8848–8855.
24 Zhang X, Goncalves R and Mosser DM (2008) The isolation and characterization of murine macrophages. *Curr Protoc Immunol* **Chapter 14**, Unit 14 1.
25 Chen L, Charrier AL, Leask A, French SW and Brigstock DR (2011) Ethanol-stimulated differentiated functions of human or mouse hepatic stellate cells are mediated by connective tissue growth factor. *J Hepatol* **55**, 399–406.
26 Huang G and Brigstock DR (2010) Integrin expression and function in the response of primary culture hepatic stellate cells to connective tissue growth factor (CCN2). *J Cell Mol Med* **15**, 1087–1095.
27 Yu MC, Chen CH, Liang X, Wang L, Gandhi CR, Fung JJ, Lu L and Qian S (2004) Inhibition of T-cell responses by hepatic stellate cells via B7-H1-mediated T-cell apoptosis in mice. *Hepatology* **40**, 1312–1321.
28 Schober JM, Chen N, Grzeszkiewicz TM, Jovanovic I, Emeson EE, Ugarova TP, Ye RD, Lau LF and Lam SC (2002) Identification of integrin alpha(M)beta(2) as an adhesion receptor on peripheral blood monocytes for Cyr61 (CCN1) and connective tissue growth factor (CCN2): immediate-early gene products expressed in atherosclerotic lesions. *Blood* **99**, 4457–4465.
29 Schober JM, Lau LF, Ugarova TP and Lam SC (2003) Identification of a novel integrin alphaMbeta2 binding site in CCN1 (CYR61), a matricellular protein expressed in healing wounds and atherosclerotic lesions. *J Biol Chem* **278**, 25808–25815.
30 Sugiyama A, Kanno K, Nishimichi N, Ohta S, Ono J, Conway SJ, Izuhara K, Yokosaki Y and Tazuma S (2016) Periostin promotes hepatic fibrosis in mice by modulating hepatic stellate cell activation via alpha integrin interaction. *J Gastroenterol* doi: 10.1007/s00535-016-1206-0.
31 Urtasun R, Lopategi A, George J, Leung TM, Lu Y, Wang X, Ge X, Fiel MI and Nieto N (2012) Osteopontin, an oxidant stress sensitive cytokine, up-regulates collagen-I via integrin alpha(V)beta(3) engagement and PI3K/pAkt/NFkappaB signaling. *Hepatology* **55**, 594–608.
32 Zhou X, Murphy FR, Gehdu N, Zhang J, Iredale JP and Benyon RC (2004) Engagement of alphavbeta3 integrin regulates proliferation and apoptosis of hepatic stellate cells. *J Biol Chem* **279**, 23996–24006.
33 Henderson NC, Arnold TD, Katamura Y, Giacomini MM, Rodriguez JD, McCarty JH, Pellicoro A, Raschperger E, Betsholtz C, Ruminski PG *et al.* (2013) Targeting of alphav integrin identifies a core molecular pathway that regulates fibrosis in several organs. *Nat Med* **19**, 1617–1624.
34 Patsenker E, Popov Y, Stickel F, Schneider V, Ledermann M, Sagesser H, Niedobitek G, Goodman SL and Schuppan D (2009) Pharmacological inhibition of integrin alphavbeta3 aggravates experimental liver fibrosis and suppresses hepatic angiogenesis. *Hepatology* **50**, 1501–1511.
35 Patsenker E and Stickel F (2011) Role of integrins in fibrosing liver diseases. *Am J Physiol Gastrointest Liver Physiol* **301**, G425–G434.
36 Pranitha P and Sudhakaran PR (2003) Fibronectin dependent upregulation of matrix metalloproteinases in hepatic stellate cells. *Indian J Biochem Biophys* **40**, 409–415.
37 Dodig M, Ogunwale B, Dasarathy S, Li M, Wang B and McCullough AJ (2007) Differences in regulation of type I collagen synthesis in primary and passaged hepatic stellate cell cultures: the role of alpha5beta1-integrin. *Am J Physiol Gastrointest Liver Physiol* **293**, G154–G164.
38 Rodriguez-Juan C, de la Torre P, Garcia-Ruiz I, Diaz-Sanjuan T, Munoz-Yague T, Gomez-Izquierdo E, Solis-Munoz P and Solis-Herruzo JA (2009) Fibronectin increases survival of rat hepatic stellate cells–a novel profibrogenic mechanism of fibronectin. *Cell Physiol Biochem* **24**, 271–282.
39 Milliano MT and Luxon BA (2003) Initial signaling of the fibronectin receptor (alpha5beta1 integrin) in hepatic stellate cells is independent of tyrosine phosphorylation. *J Hepatol* **39**, 32–37.
40 Wang R, Ding Q, Yaqoob U, de Assuncao TM, Verma VK, Hirsova P, Cao S, Mukhopadhyay D, Huebert RC and Shah VH (2015) Exosome adherence and internalization by hepatic stellate cells triggers sphingosine 1-phosphate-dependent migration. *J Biol Chem* **290**, 30684–30696.

41 Levine D, Rockey DC, Milner TA, Breuss JM, Fallon JT and Schnapp LM (2000) Expression of the integrin alpha8beta1 during pulmonary and hepatic fibrosis. *Am J Pathol* **156**, 1927–1935.
42 Carloni V, Romanelli RG, Pinzani M, Laffi G and Gentilini P (1996) Expression and function of integrin receptors for collagen and laminin in cultured human hepatic stellate cells. *Gastroenterology* **110**, 1127–1136.
43 Segura E, Guerin C, Hogg N, Amigorena S and Thery C (2007) CD8 + dendritic cells use LFA-1 to capture MHC-peptide complexes from exosomes in vivo. *J Immunol* **179**, 1489–1496.
44 Nolte-'t Hoen EN, Buschow SI, Anderton SM, Stoorvogel W and Wauben MH (2009) Activated T Cells Recruit Exosomes Secreted by Dendritic Cells via LFA-1. *Blood* **113**, 1977–1981.
45 Wubbolts R, Leckie RS, Veenhuizen PT, Schwarzmann G, Mobius W, Hoernschemeyer J, Slot JW, Geuze HJ and Stoorvogel W (2003) Proteomic and biochemical analyses of human B cell-derived exosomes. Potential implications for their function and multivesicular body formation. *J Biol Chem* **278**, 10963–10972.
46 Rieu S, Geminard C, Rabesandratana H, Sainte-Marie J and Vidal M (2000) Exosomes released during reticulocyte maturation bind to fibronectin via integrin alpha4beta1. *Eur J Biochem* **267**, 583–590.
47 Thery C, Boussac M, Veron P, Ricciardi-Castagnoli P, Raposo G, Garin J and Amigorena S (2001) Proteomic analysis of dendritic cell-derived exosomes: a secreted subcellular compartment distinct from apoptotic vesicles. *J Immunol* **166**, 7309–7318.
48 Thery C, Regnault A, Garin J, Wolfers J, Zitvogel L, Ricciardi-Castagnoli P, Raposo G and Amigorena S (1999) Molecular characterization of dendritic cell-derived exosomes. Selective accumulation of the heat shock protein hsc73. *J Cell Biol* **147**, 599–610.
49 Clayton A, Turkes A, Dewitt S, Steadman R, Mason MD and Hallett MB (2004) Adhesion and signaling by B cell-derived exosomes: the role of integrins. *FASEB J* **18**, 977–979.
50 Janowska-Wieczorek A, Wysoczynski M, Kijowski J, Marquez-Curtis L, Machalinski B, Ratajczak J and Ratajczak MZ (2005) Microvesicles derived from activated platelets induce metastasis and angiogenesis in lung cancer. *Int J Cancer* **113**, 752–760.
51 Kawakami K, Fujita Y, Kato T, Mizutani K, Kameyama K, Tsumoto H, Miura Y, Deguchi T and Ito M (2015) Integrin beta4 and vinculin contained in exosomes are potential markers for progression of prostate cancer associated with taxane-resistance. *Int J Oncol* **47**, 384–390.
52 Fedele C, Singh A, Zerlanko BJ, Iozzo RV and Languino LR (2015) The alphavbeta6 integrin is transferred intercellularly via exosomes. *J Biol Chem* **290**, 4545–4551.
53 Hoshino A, Costa-Silva B, Shen TL, Rodrigues G, Hashimoto A, Tesic Mark M, Molina H, Kohsaka S, Di Giannatale A, Ceder S *et al*. (2015) Tumour exosome integrins determine organotropic metastasis. *Nature* **527**, 329–335.
54 Belting M (2003) Heparan sulfate proteoglycan as a plasma membrane carrier. *Trends Biochem Sci* **28**, 145–151.
55 Kreuger J, Spillmann D, Li JP and Lindahl U (2006) Interactions between heparan sulfate and proteins: the concept of specificity. *J Cell Biol* **174**, 323–327.
56 Bishop JR, Schuksz M and Esko JD (2007) Heparan sulphate proteoglycans fine-tune mammalian physiology. *Nature* **446**, 1030–1037.
57 Dreyfuss JL, Regatieri CV, Jarrouge TR, Cavalheiro RP, Sampaio LO and Nader HB (2009) Heparan sulfate proteoglycans: structure, protein interactions and cell signaling. *An Acad Bras Cienc* **81**, 409–429.
58 Sarrazin S, Lamanna WC and Esko JD (2011) Heparan sulfate proteoglycans. *Cold Spring Harb Perspect Biol* **3**, pii: a004952.
59 Safaiyan F, Kolset SO, Prydz K, Gottfridsson E, Lindahl U and Salmivirta M (1999) Selective effects of sodium chlorate treatment on the sulfation of heparan sulfate. *J Biol Chem* **274**, 36267–36273.
60 Keller KM, Brauer PR and Keller JM (1989) Modulation of cell surface heparan sulfate structure by growth of cells in the presence of chlorate. *Biochemistry* **28**, 8100–8107.
61 Gao R and Brigstock DR (2003) Low density lipoprotein receptor-related protein (LRP) is a heparin-dependent adhesion receptor for connective tissue growth factor (CTGF) in rat activated hepatic stellate cells. *Hepatol Res* **27**, 214–220.
62 Christianson HC, Svensson KJ, van Kuppevelt TH, Li JP and Belting M (2013) Cancer cell exosomes depend on cell-surface heparan sulfate proteoglycans for their internalization and functional activity. *Proc Natl Acad Sci USA* **110**, 17380–17385.
63 Roskams T, Rosenbaum J, De Vos R, David G and Desmet V (1996) Heparan sulfate proteoglycan expression in chronic cholestatic human liver diseases. *Hepatology* **24**, 524–532.
64 Beljaars L, Molema G, Schuppan D, Geerts A, De Bleser PJ, Weert B, Meijer DK and Poelstra K (2000) Successful targeting to rat hepatic stellate cells using albumin modified with cyclic peptides that recognize the collagen type VI receptor. *J Biol Chem* **275**, 12743–12751.
65 Huang XW, Wang JY, Li F, Song ZJ, Xie C and Lu WY (2010) Biochemical characterization of the binding of cyclic RGDyK to hepatic stellate cells. *Biochem Pharmacol* **80**, 136–143.
66 Brigstock DR (2009) Strategies for blocking the fibrogenic actions of connective tissue growth factor (CCN2): from pharmacological inhibition in vitro to targeted siRNA therapy in vivo. *J Cell Commun Signal* **3**, 5–18.